



Supplementary Information for Part 1

Three mutations repurpose a plant karrikin receptor to a strigolactone receptor

Amir Arellano-Saab^{1,6}, Michael Bunsick¹, Hasan Al Galib¹, Wenda Zhao¹, Stefan Schuetz¹, James Michael Bradley¹, Zhenhua Xu¹, Claresta Adityani¹, Asrinus Subha¹, Hayley McKay¹, Alexandre de Saint Germain², François-Didier Boyer³, Christopher S. P. McErlan⁴, Shigeo Toh⁵, Peter McCourt¹, Peter J. Stogios^{6,7} and Shelley Lumba^{1,7}

Email: shelley.lumba@utoronto.ca
peter.stogios@utoronto.ca
peter.mccourt@utoronto.ca

This PDF file includes:

Figures S1 to S11

Tables S1 to S3

Legends for Movies S1 to S3

Other supplementary materials for this manuscript include the following:

Movies S1 to S3

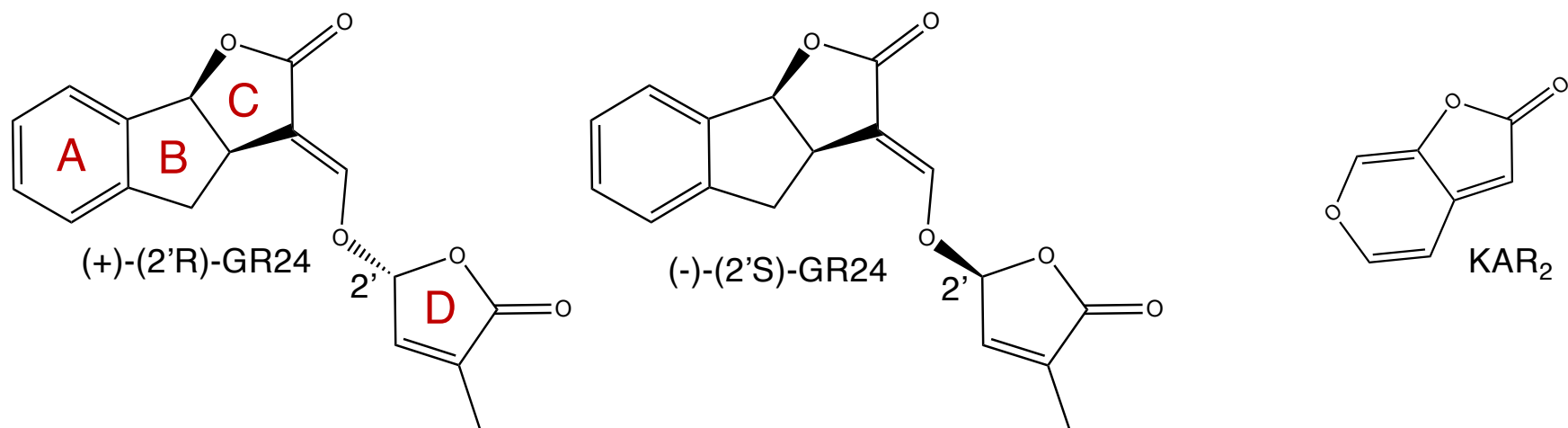


Fig. S1. Structures of 2'R- and 2S'-enantiomeric forms of strigolactones (SLs) and karrikin (KAR₂). For SLs the synthetic GR24 is shown and the 2' chirality is at the enol-ether bridge between the C and D-ring. For karrikin KAR₂ is shown.

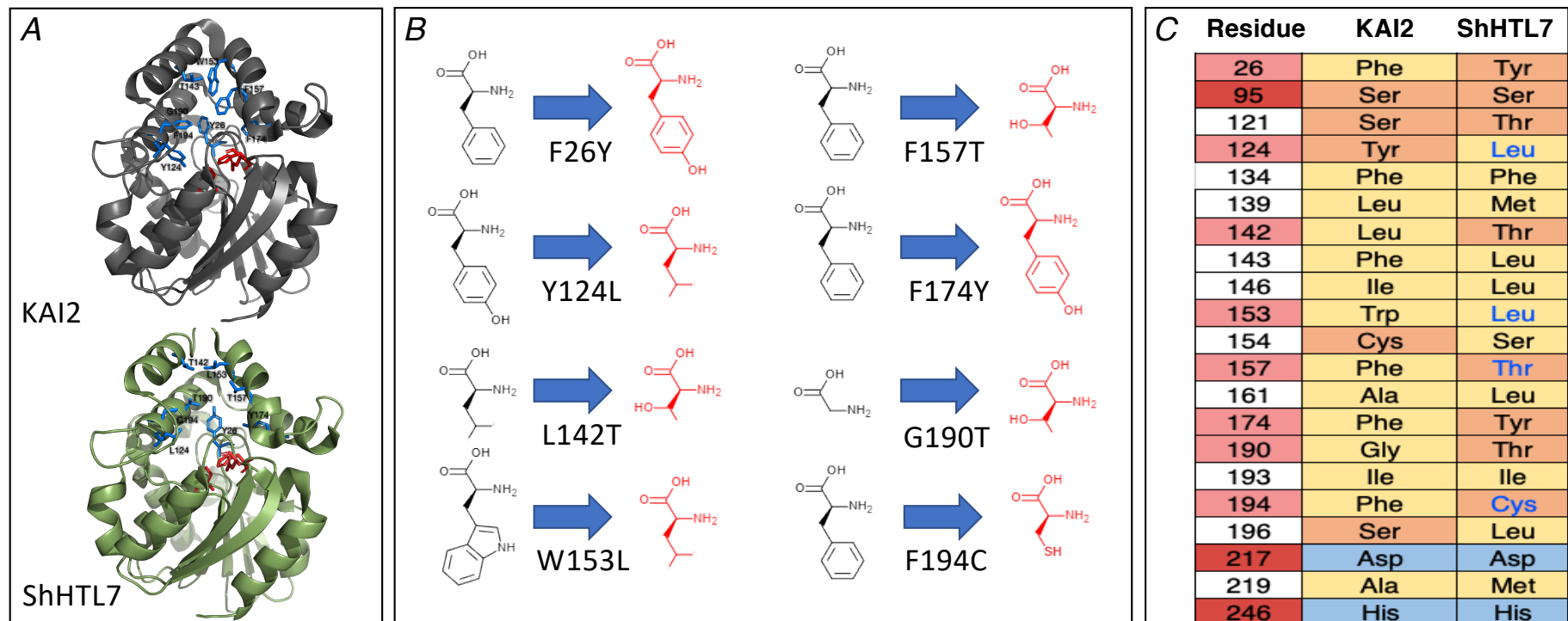


Fig. S2. Selection of eight ShHTL7 residues for substitution in KAI2. (A) Crystal structures representing the eight residues highlighted in blue, The three catalytic residues highlighted in red. Structures are visualized using PYMOL version 2.3.2. (B) Chemical structures of the amino acids at the positions substituted in KAI2 to generate JGI variants. Structures in black represent the amino acids present at these positions in KAI2, structures in red represent their counterparts in ShHTL7. Letter codes and numbers below the arrows denote the substitutions that were made to produce the JGI variants. (C) The choice of the eight substitutions (pink boxes) were made based on increased polarity and decreased size (blue amino acids) in ShHTL7 versus the KAI2 equivalent. Red boxes represent the three catalytic residues.

■ Catalytic triad
■ Substitution residues
■ Polar side chain
■ Non-Polar side chain
■ Electrically charged side chain

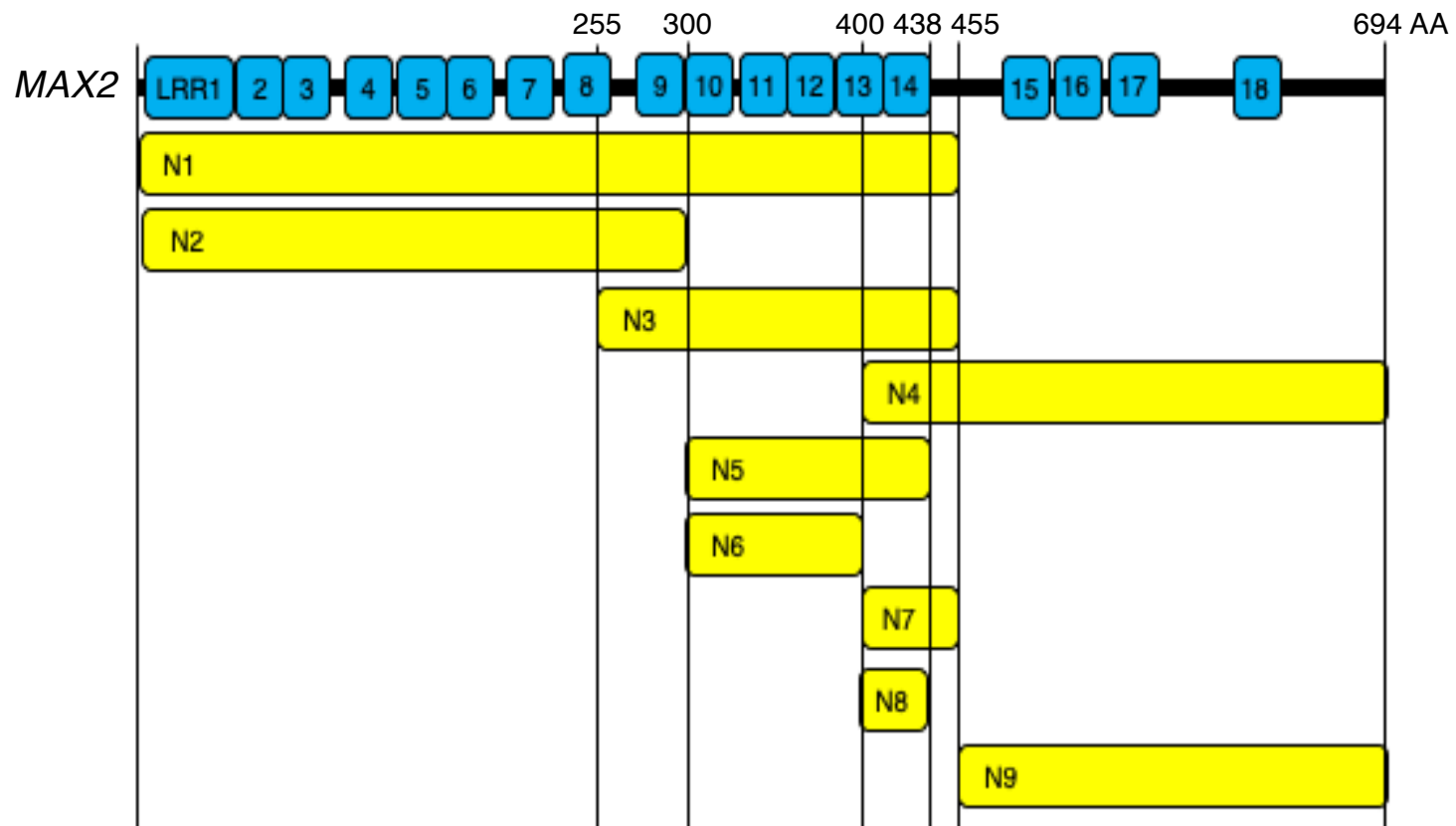


Fig. S3. Map of MAX2 fragments used in yeast-two-hybrid (Y2H) experiments.

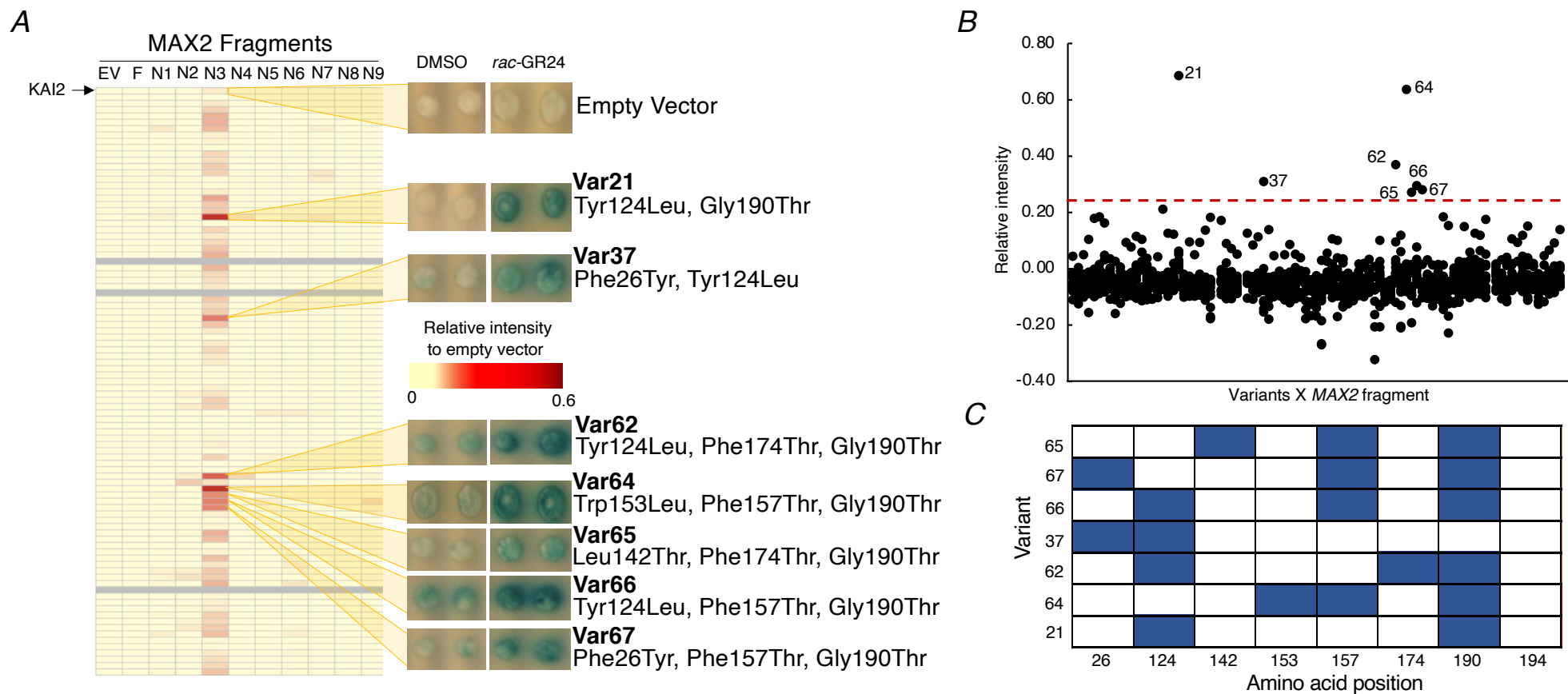
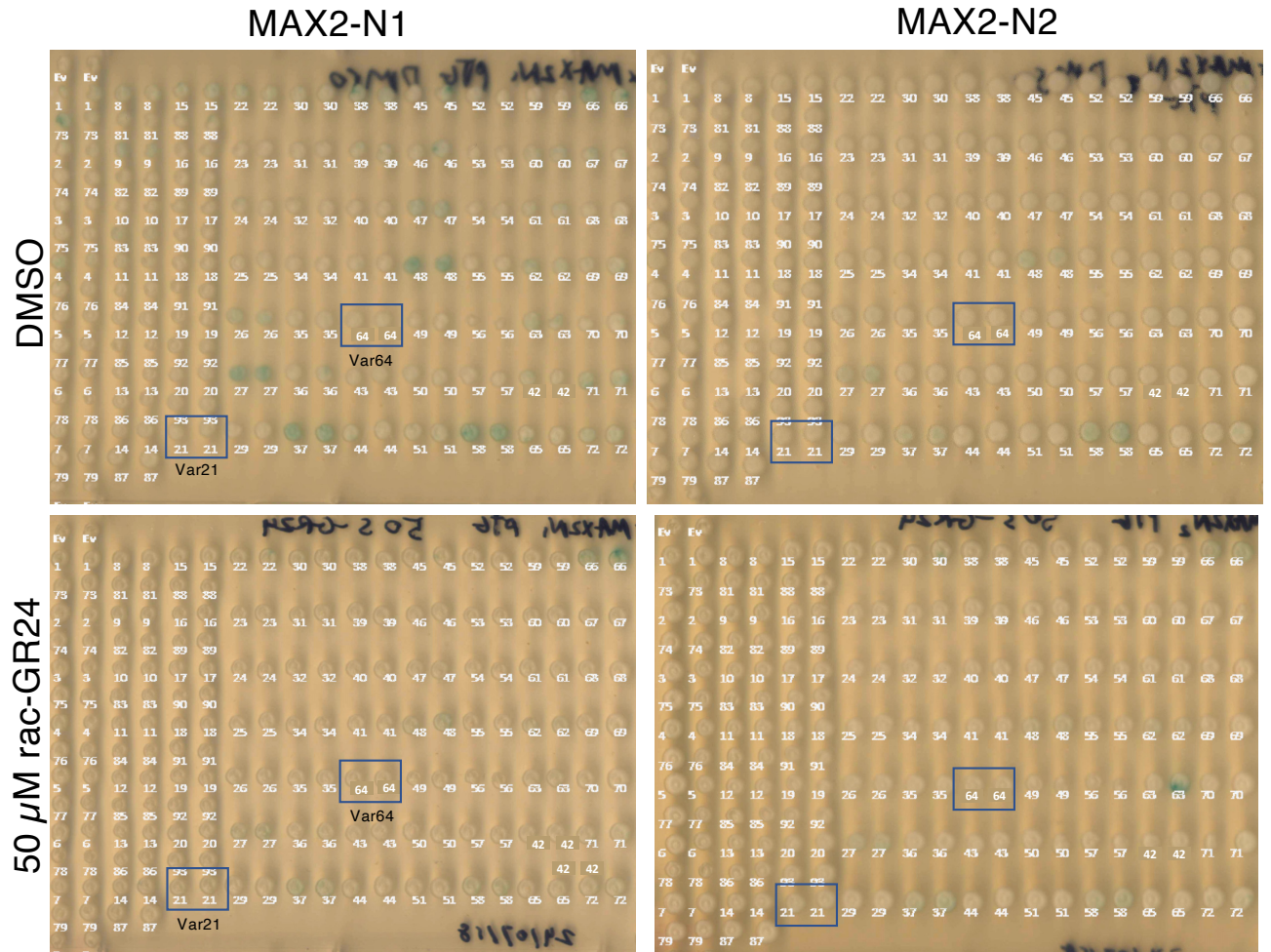


Fig. S4. Yeast-two hybrid interactions of KAI2 variants with MAX2 (A) Heatmap of log-fold change scores based on interactions relative to DMSO conditions queried against all MAX2 fragments (see Fig. S3). EV, empty vector, F, full-length protein, N, fragments shown in Fig. S3. Red shading indicates increased interaction, with the seven strongest interactions (Var21, 37, 62, 64, 65, 66, 67) shown. Grey lines, construct that could not be cloned. (B) Scatterplot showing the log-fold change scores calculated for each combination of an individual mis-expressed *KAI2* chimeric variant with full-length, MAX2 fragments and empty vector control based on Y2H interaction intensities. (C) Table of statistically significant hits in Y2H screen.

Fig. S5. Images of Yeast 2-hybrid (Y2H) interactions used to generate the Y2H heat map shown in **Fig. 1**. Ev is an empty vector colony. Each duplicate variant colony has its number beneath it. The two blue boxes represent Var21 and Var64.



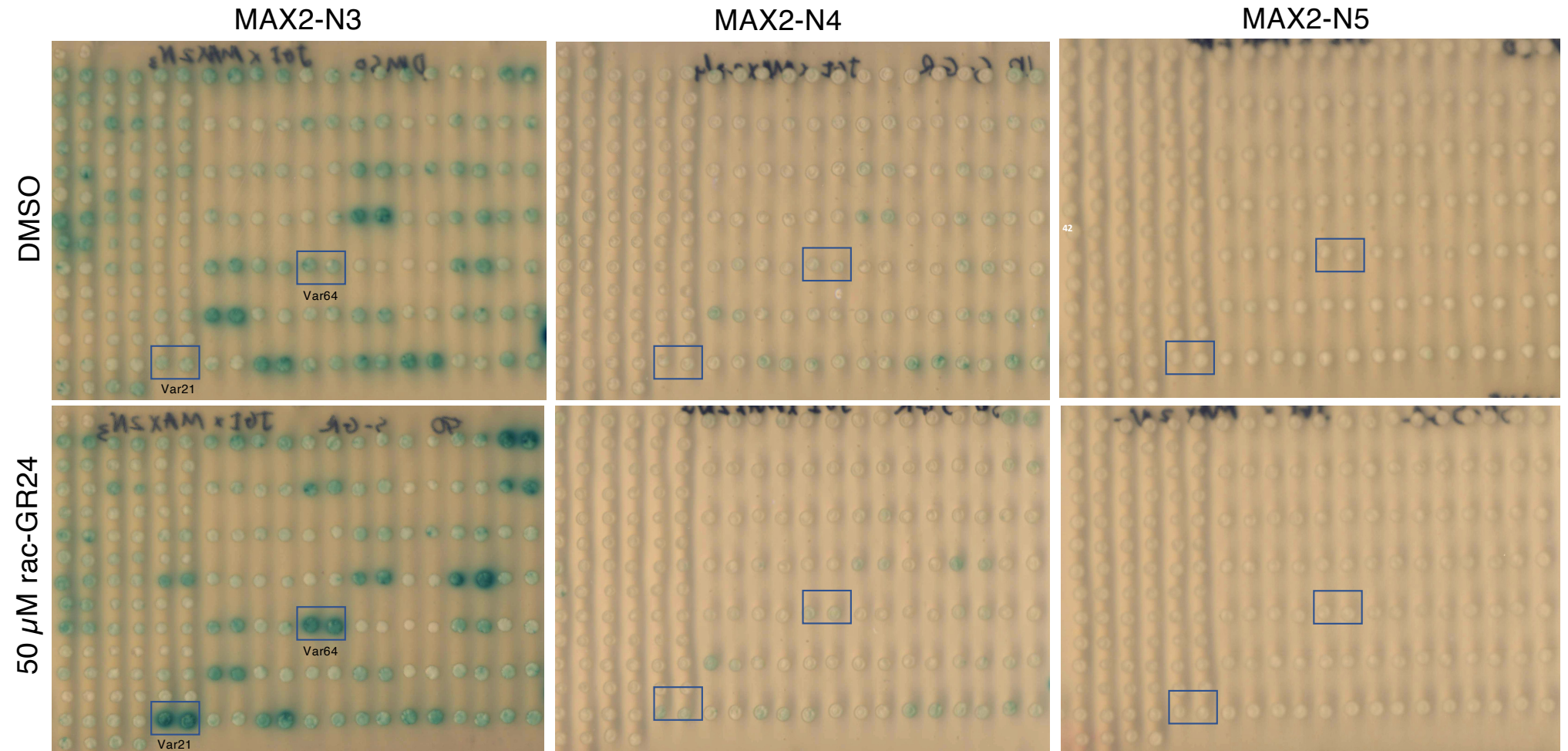


Fig. S5. Cont'd

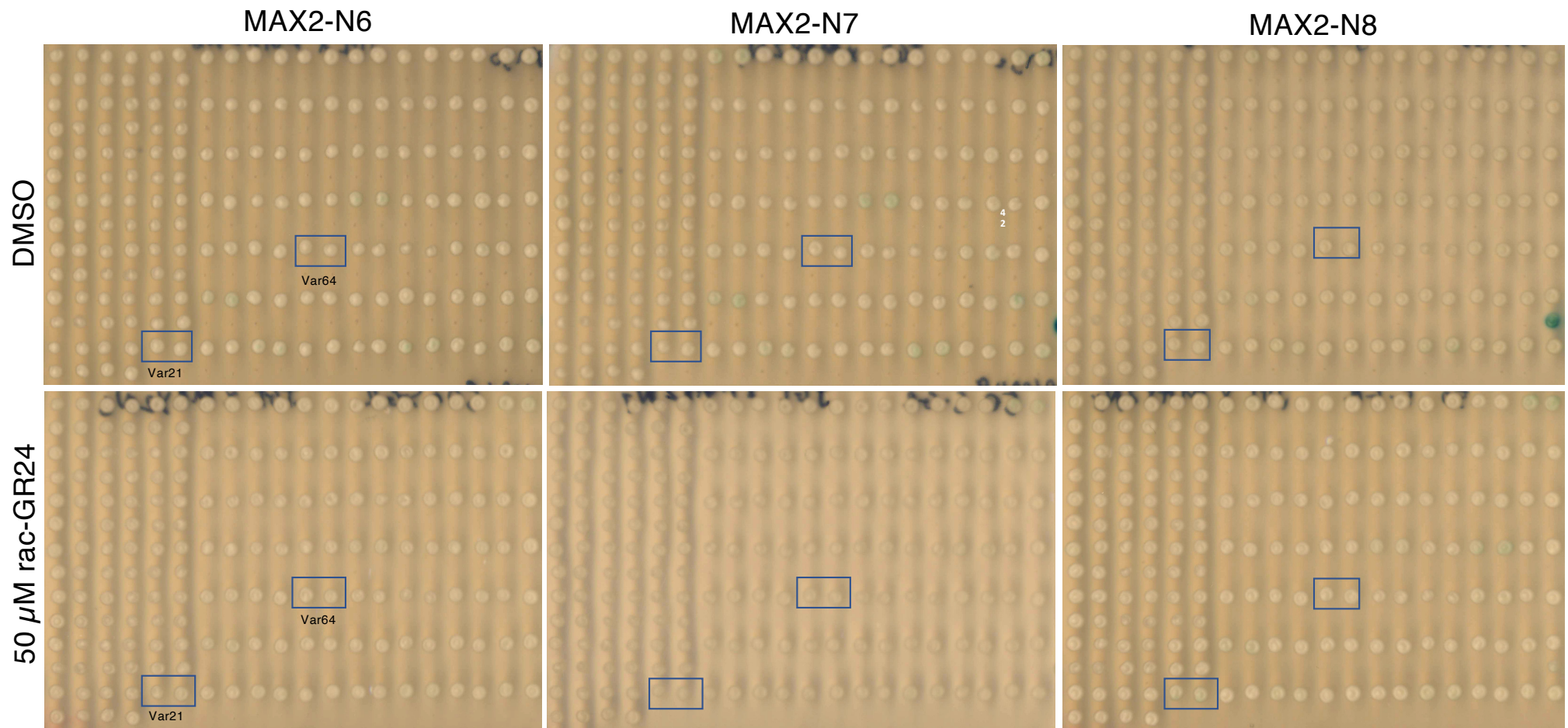


Fig. S5. Cont'd

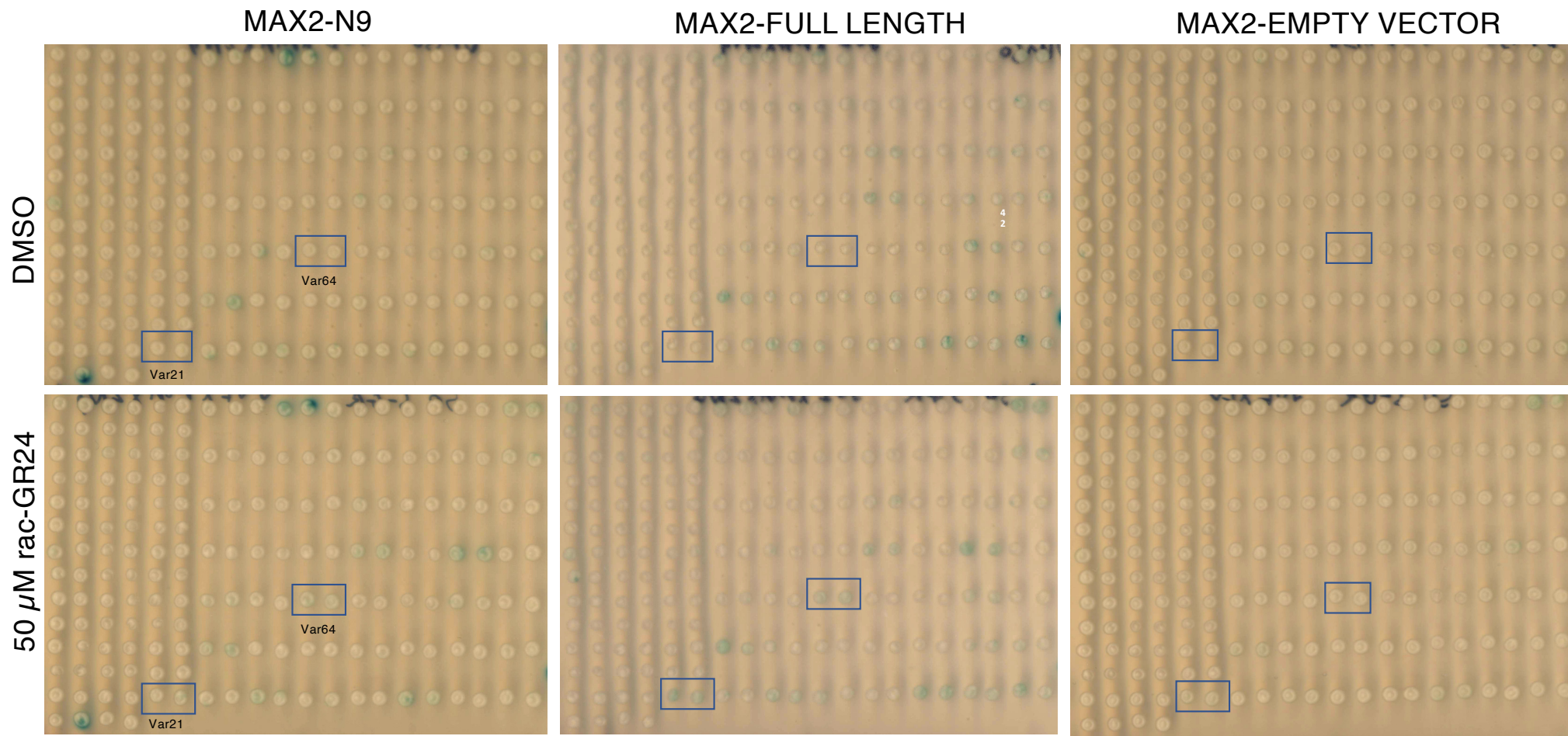


Fig. S5. Cont'd

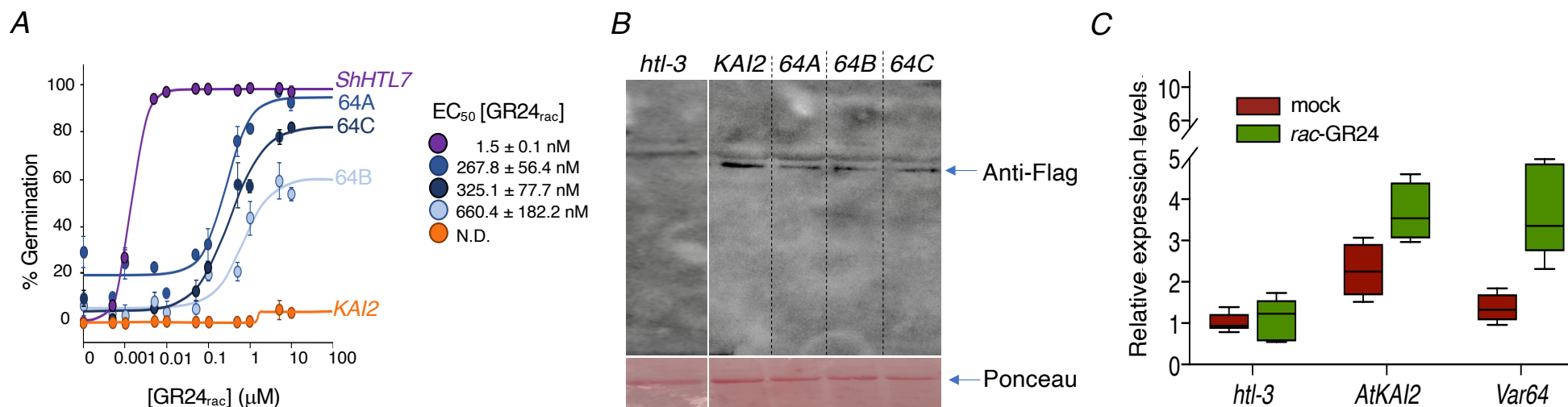


Fig. S6. Characterization of three independent Var64 transgenic lines. (A) Percent germination of mis-expressed *ShHTL7*, *KAI2* and three independent Var64 seed (64A, 64B, 64C) on PAC (20 μM) and increasing *rac*-GR24 concentrations. Four-parameter logistic curves were fitted to the data, and EC₅₀ values, ± standard error, of *rac*-GR24 concentrations have been included for those lines showing a response on SL. Based on these curves, the effective concentration that germinates 50% of seed (EC₅₀) was calculated. (B) Western blot analysis of expression of mis-expressed *KAI2* and three independent Var64 seed (64A, 64B, 64C). Mis-expressed genes were Flag tagged and probed with an Anti-flag antibody. Ponceau staining indicates equal loading. (C) Quantitative PCR (qPCR) of *KUF1* transcripts of germinated (24 hrs) seeds in the light on PAC in the absence or presence of *rac*-GR24. Each point represents a biological replicate and each sample represents three replicates. qPCR primers *AtKUF1F* (ATTGTTGTGGTGGATGTTG), *AtKUF1R* (ATTCGGTTGACTCATTCTTG), *AtACT8F* (CCACGAGACAACCTTACAAC), *AtACT8R* (TGCCACGACCTTAATCTT). Expression values are relative to the At2g20000 reference gene. Bar=SD.

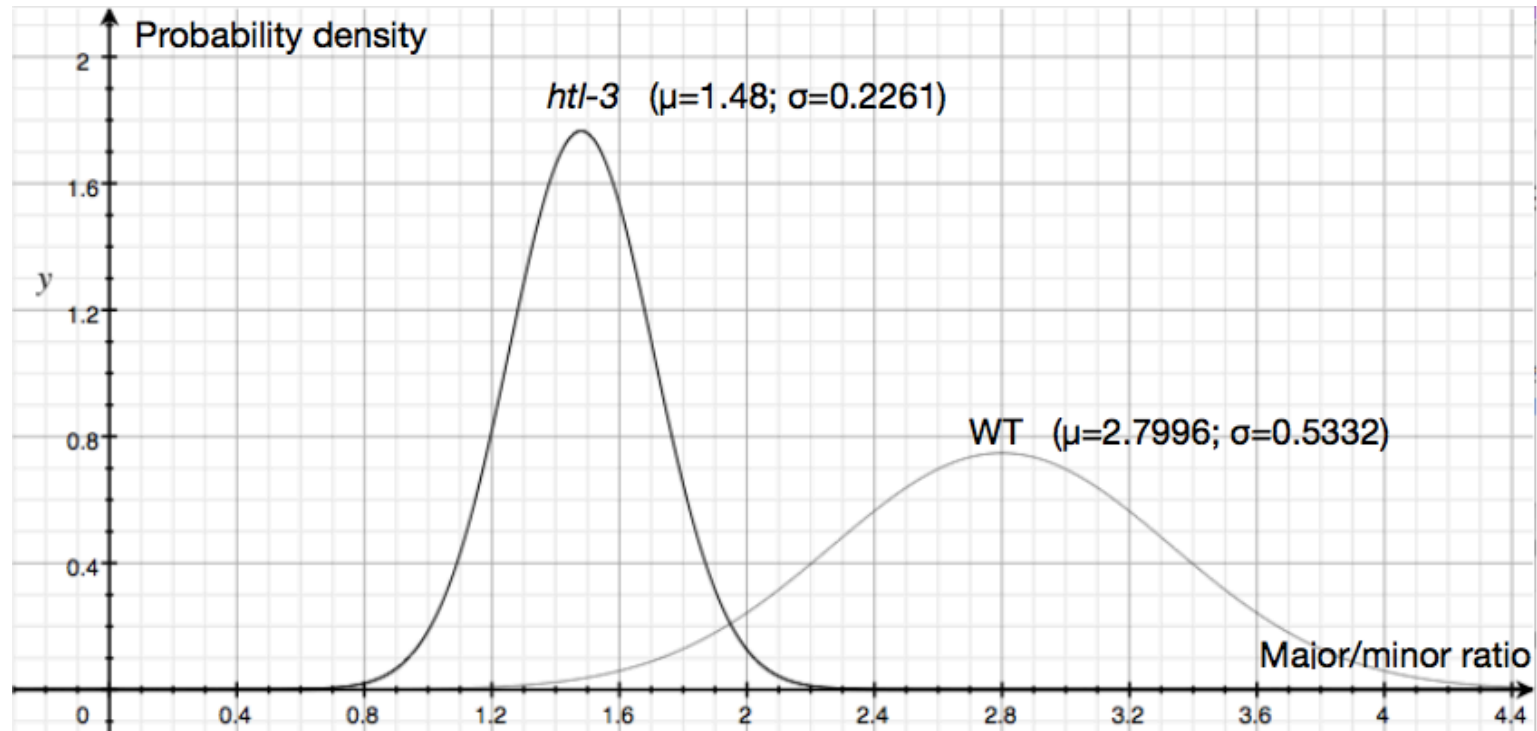


Fig. S7. Standard distribution of length/width (major/minor) ratio of *htl-3* and wild type Columbia (WT) leaves. Each distribution was a normal distribution based on the population mean (μ) and standard deviation (σ) approximated by that of the 26 control samples. WT: $y = (1 / (0.53332 \cdot \sqrt{2\pi})) \cdot e^{-x - 2.7996)^2 / (2 \cdot (0.53332)^2)}$; *htl-3*: $y = (1 / (0.2261 \cdot \sqrt{2\pi})) \cdot e^{-x - 1.48)^2 / (2 \cdot (0.2261)^2)}$. Three categories given by 5% cutoff: *htl-3*: $x < 1.85$; WT: $x > 1.92$; ambiguous: $1.85 < x < 1.92$. Based on the two distributions, in order to meet the 0.05 significance level, any sample data smaller than 1.85 would be considered as *htl-3*, while sample data larger than 1.92 would be considered as wild type. Note that there is an ambiguous region in between (1.82-1.92) where the phenotype can not be statistically determined in this case.

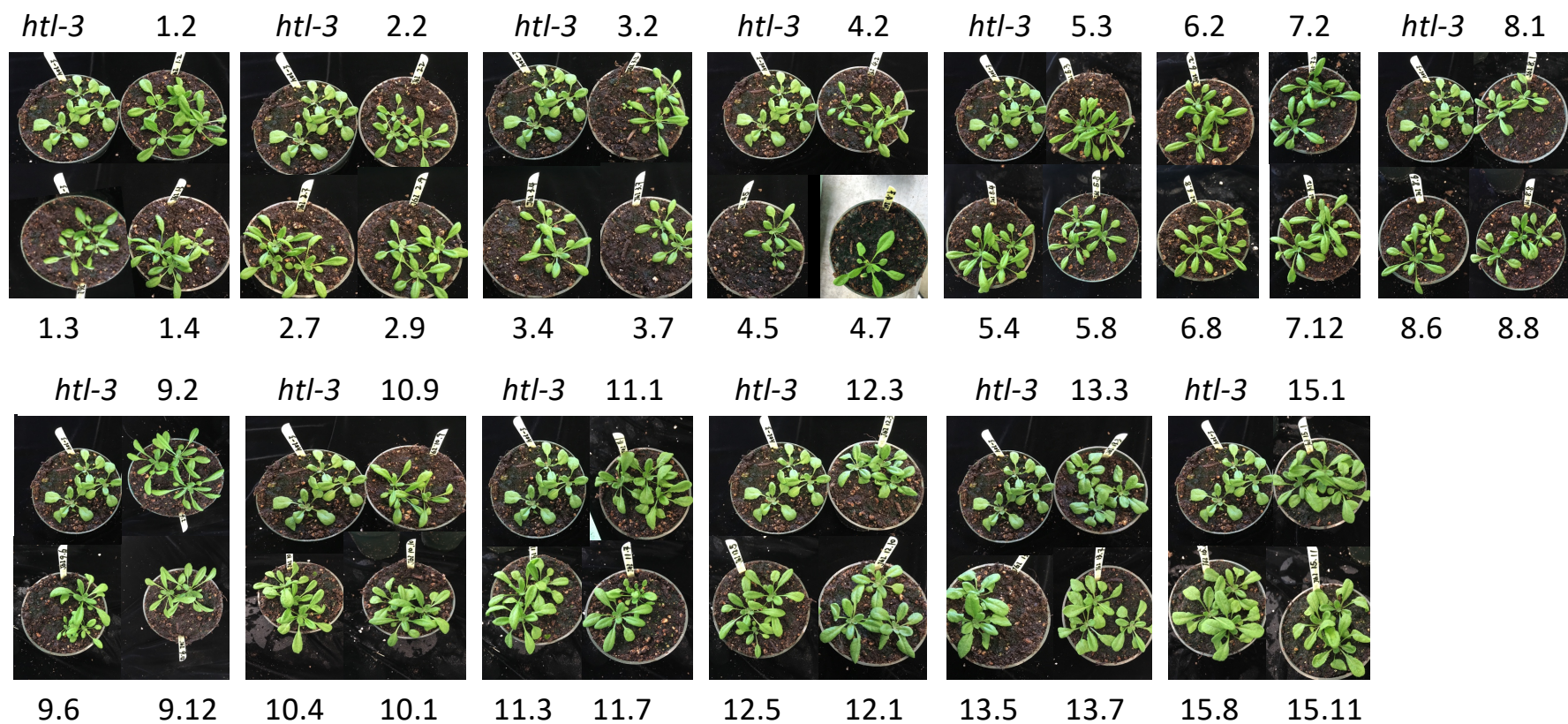


Fig. S8. Images and quantification of transgenic variant lines used to generate **Fig. 1C**. Independent lines of Var19 and Var64 are highlighted.

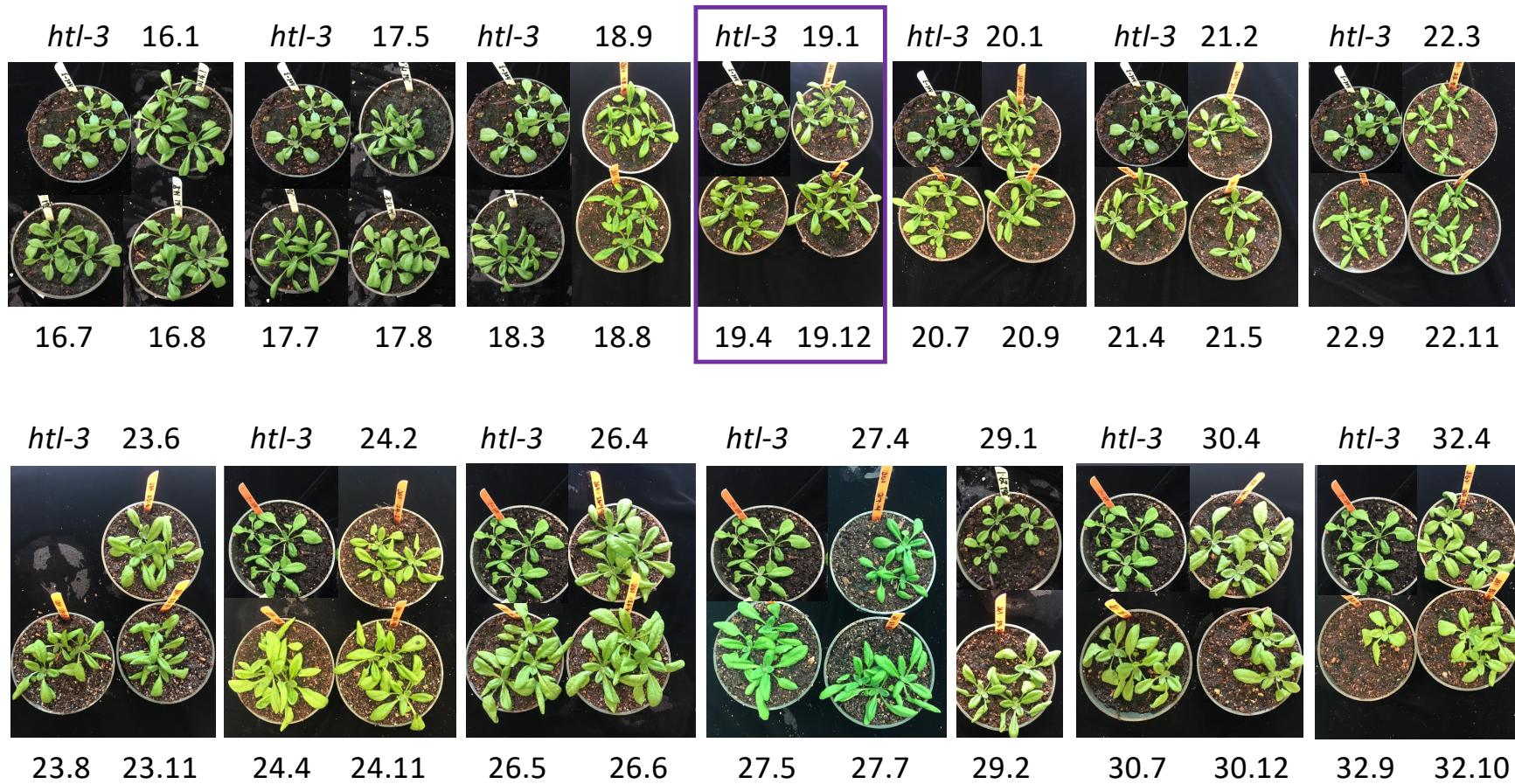


Fig. S8. Con't

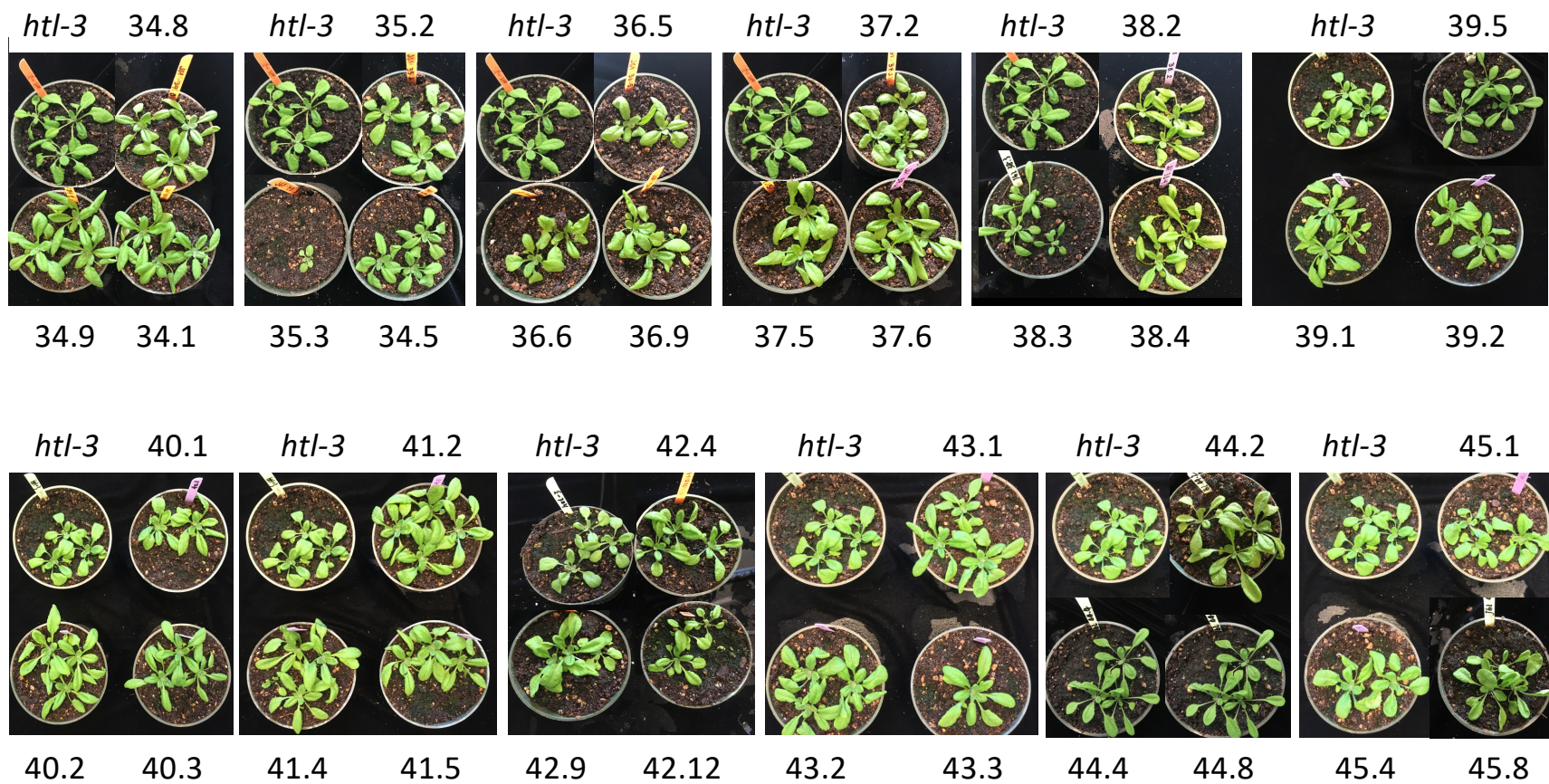


Fig. S8. Cont'd

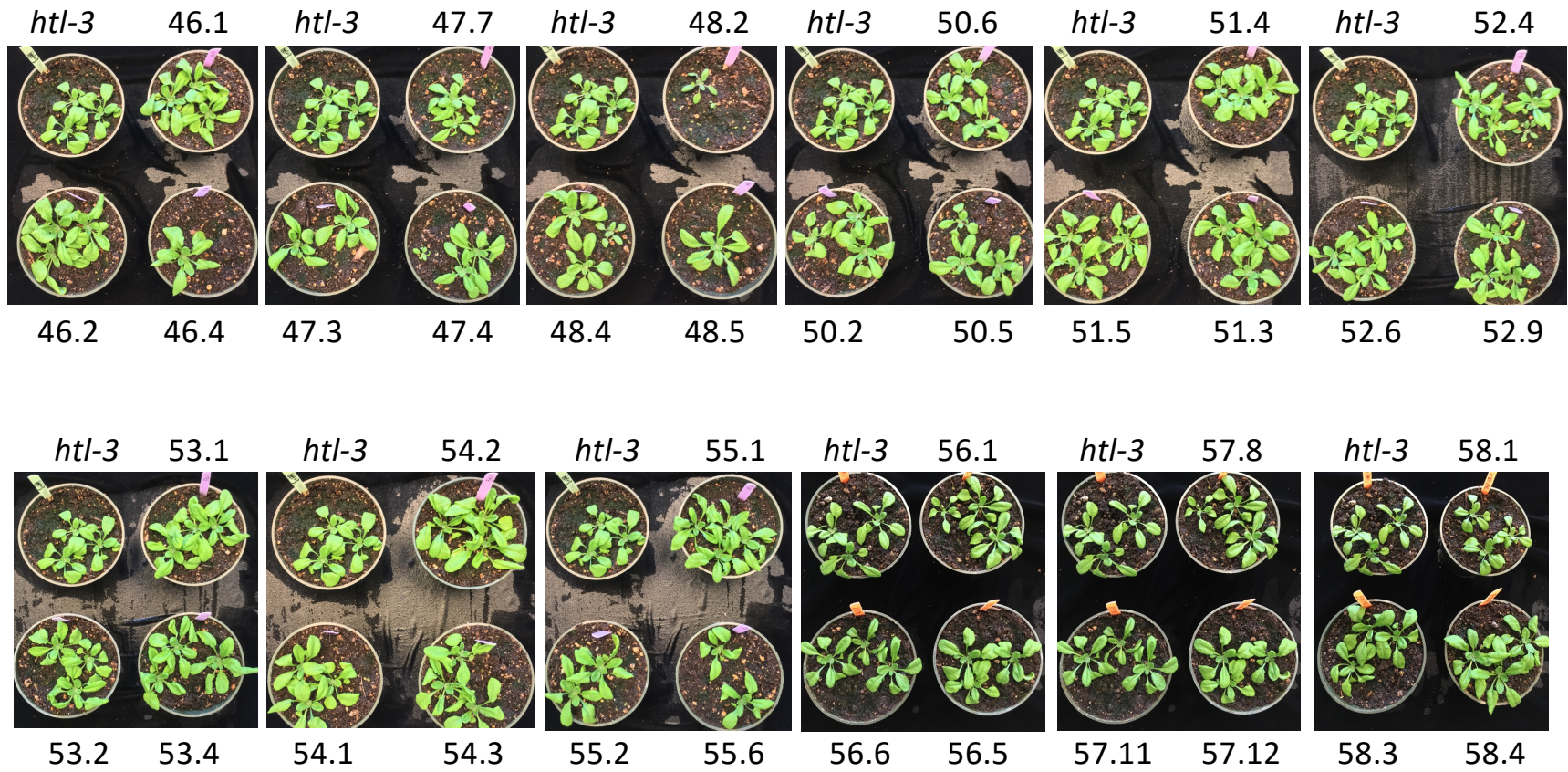


Fig. S8. Cont'd

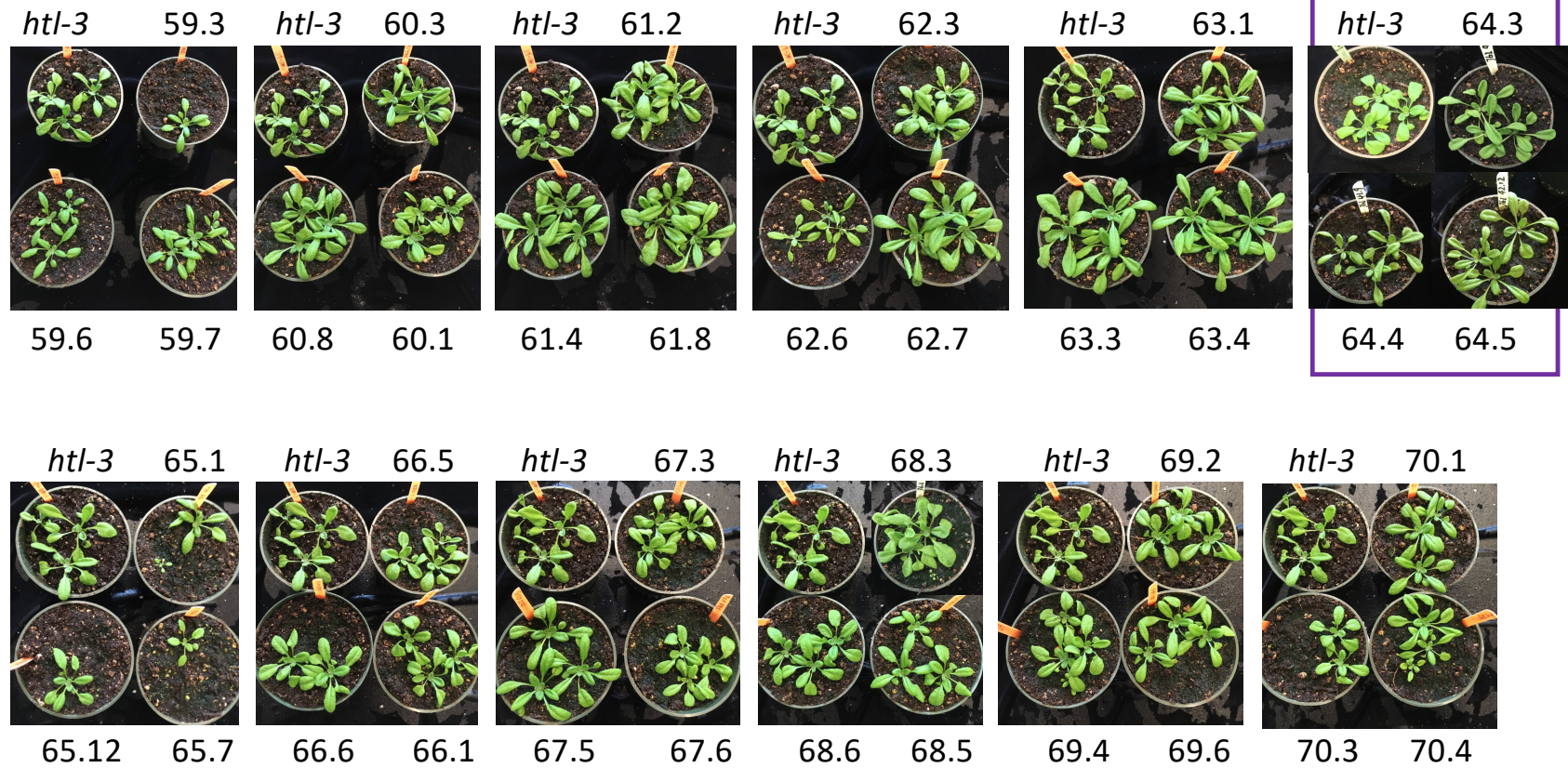


Fig. S8. Cont'd

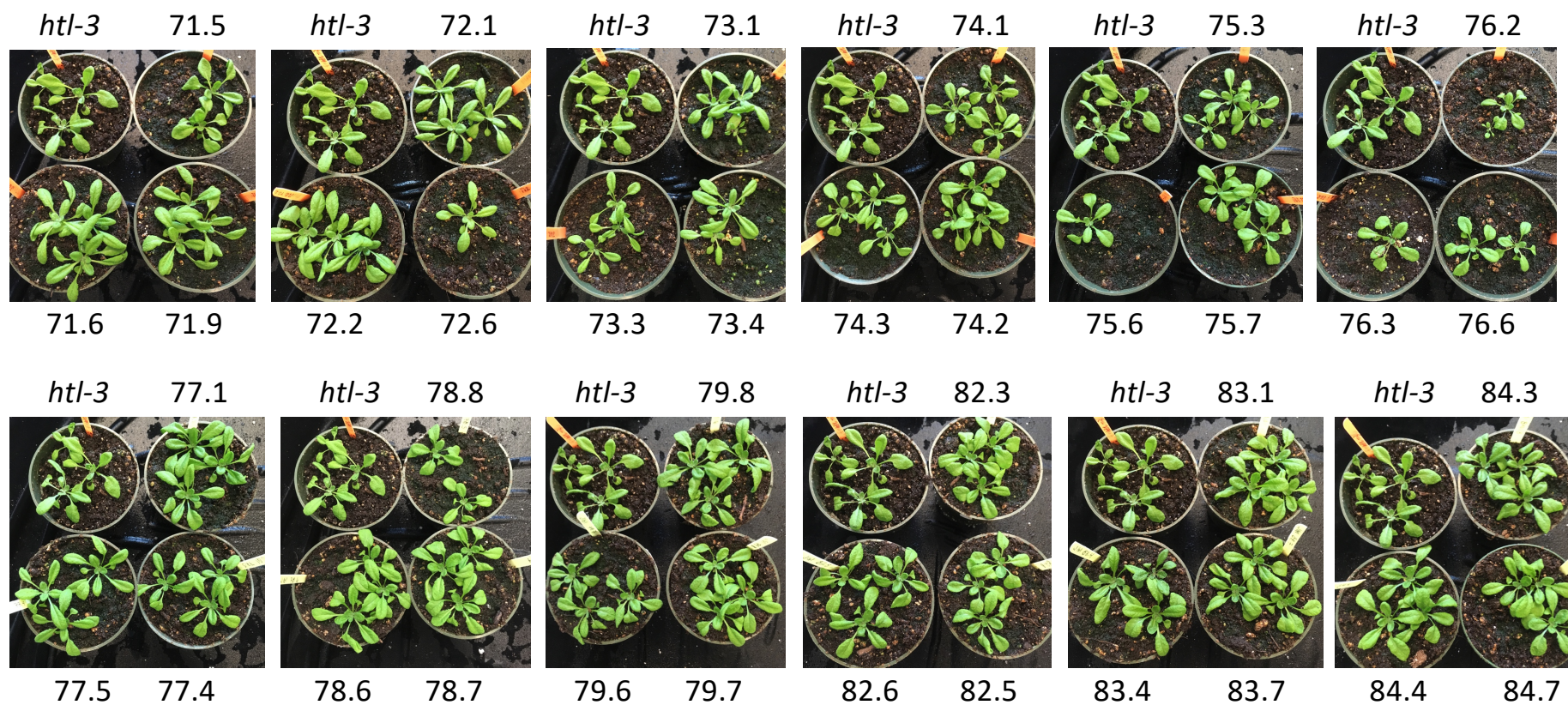


Fig. S8. Cont'd

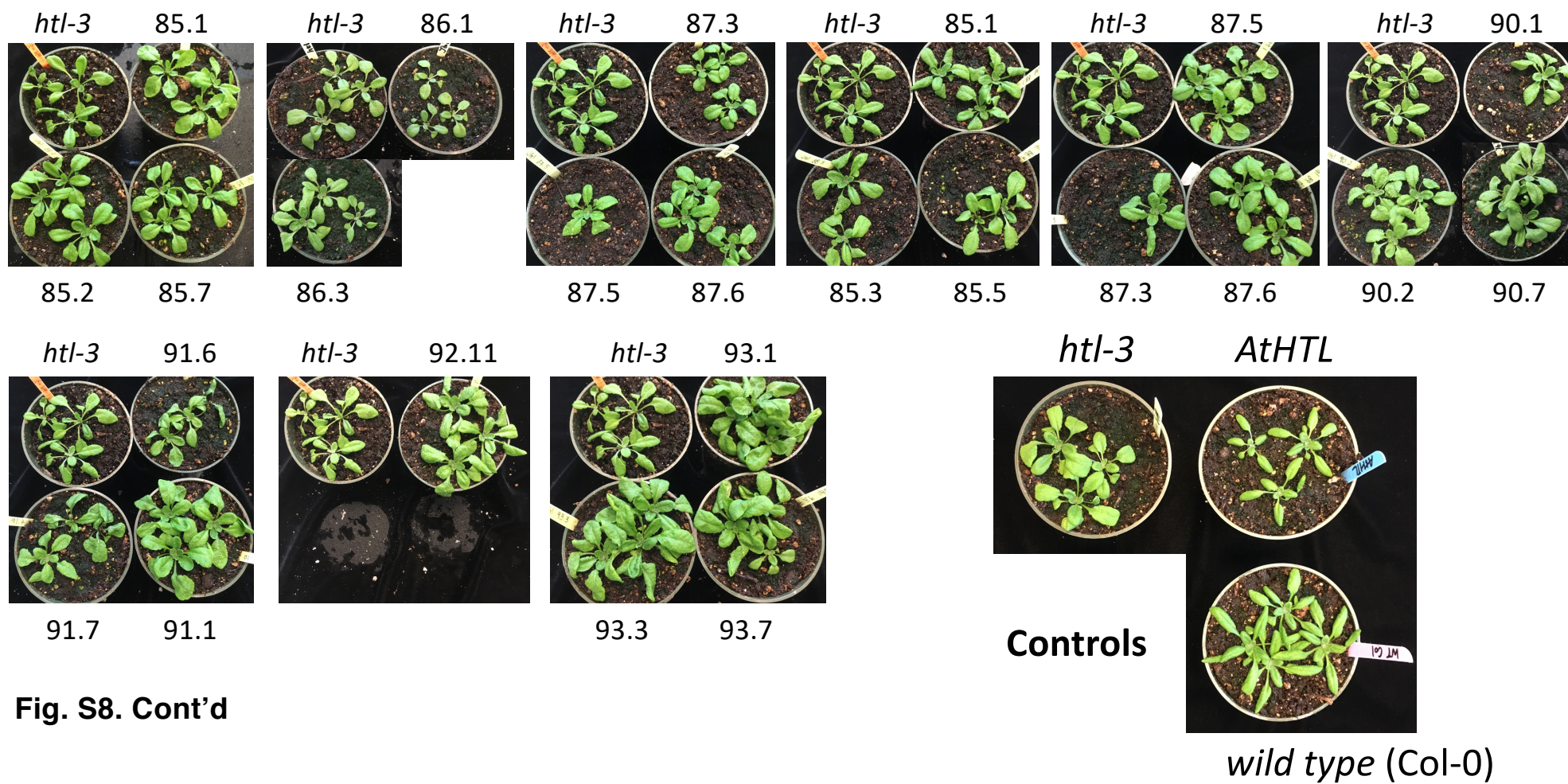


Fig. S8. Cont'd

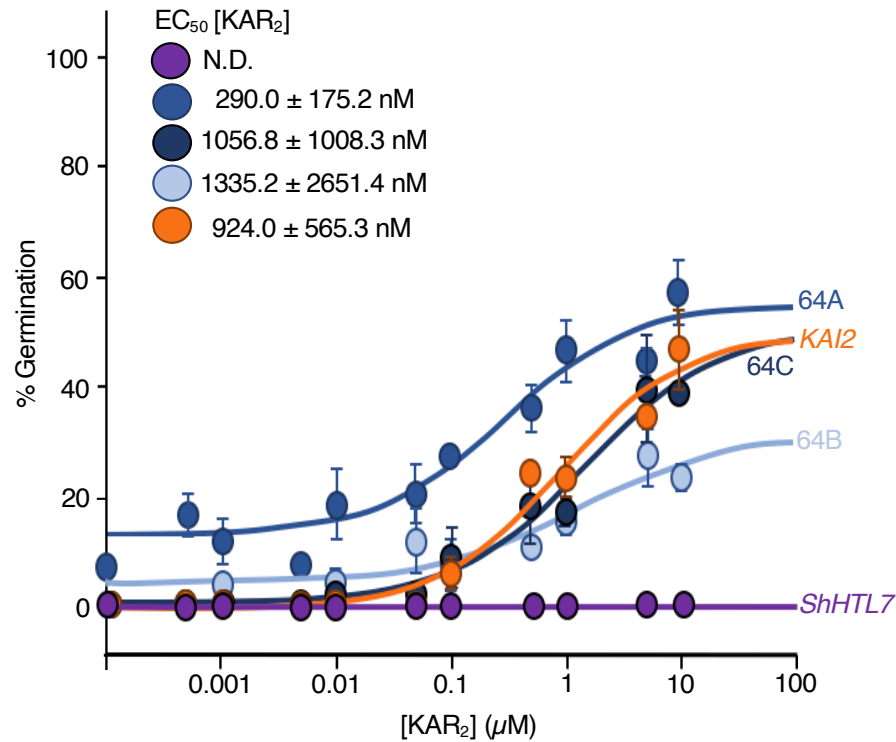


Fig. S9. Germination response of *ShHTL7*, *KAI2*, and *Var64* seed to karrikin. Misexpressed *ShHTL7*, *KAI2* and three biological independent *Var64* seed (64A, 64B, 64C) germinated on PAC (20 μM) and increasing KAR₂ concentrations. Four-parameter logistic curves were fitted to the data, and EC₅₀ values, ± standard error, of KAR₂ concentrations have been included for those lines showing response to karrikin. Based on these curves, the effective concentrations that germinates 50% of seed (EC₅₀) are indicated.

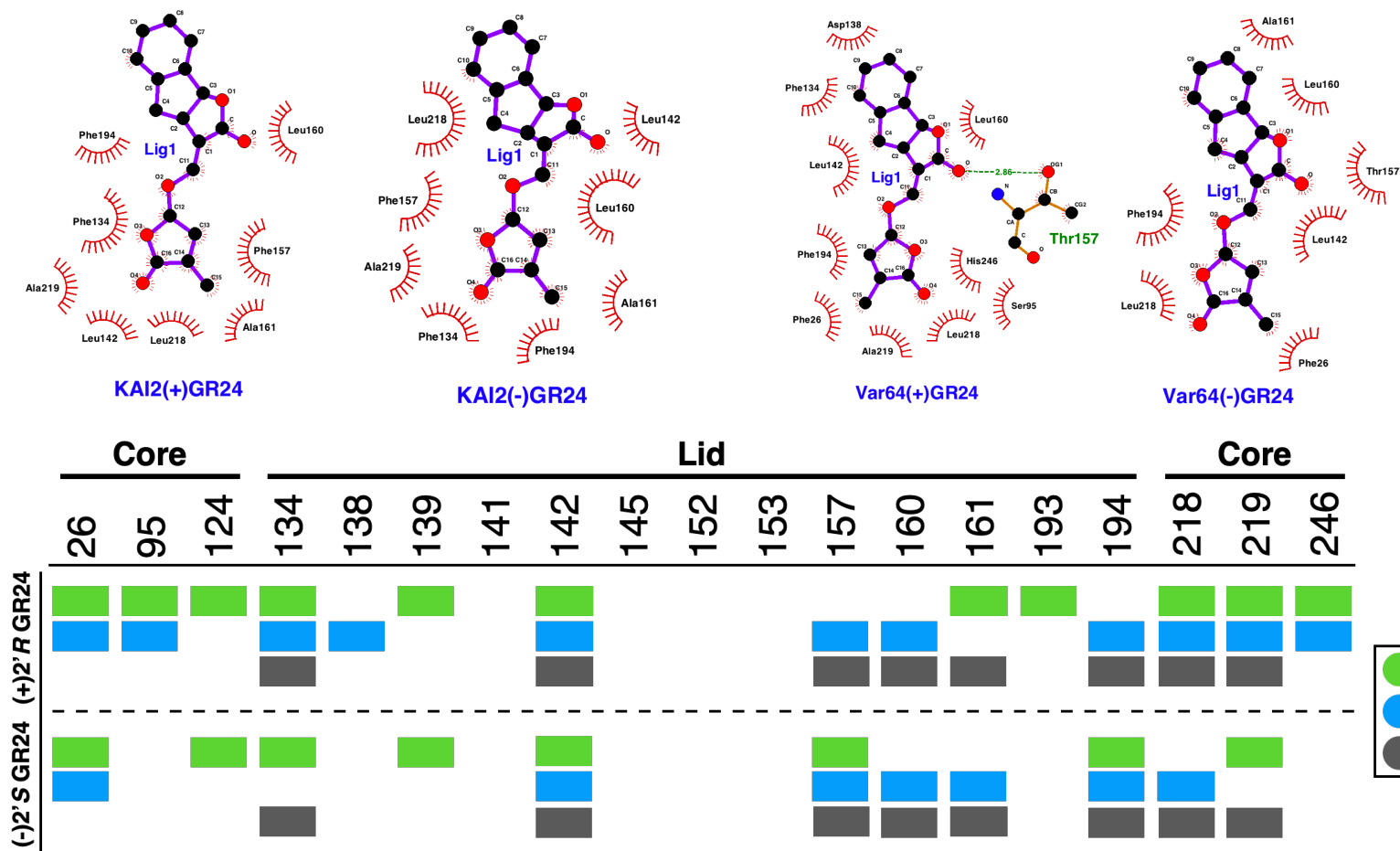


Fig. S10. *In silico* docking of *2'R*-GR24 and *2'S*-GR24. The two GR24 enantiomers were docked into ShHTL7, Var64, and KAI2. As expected, ShHTL7 displays the most interactions with *2'R*-GR24. KAI2 has the most contacts with *2'S*-GR24.

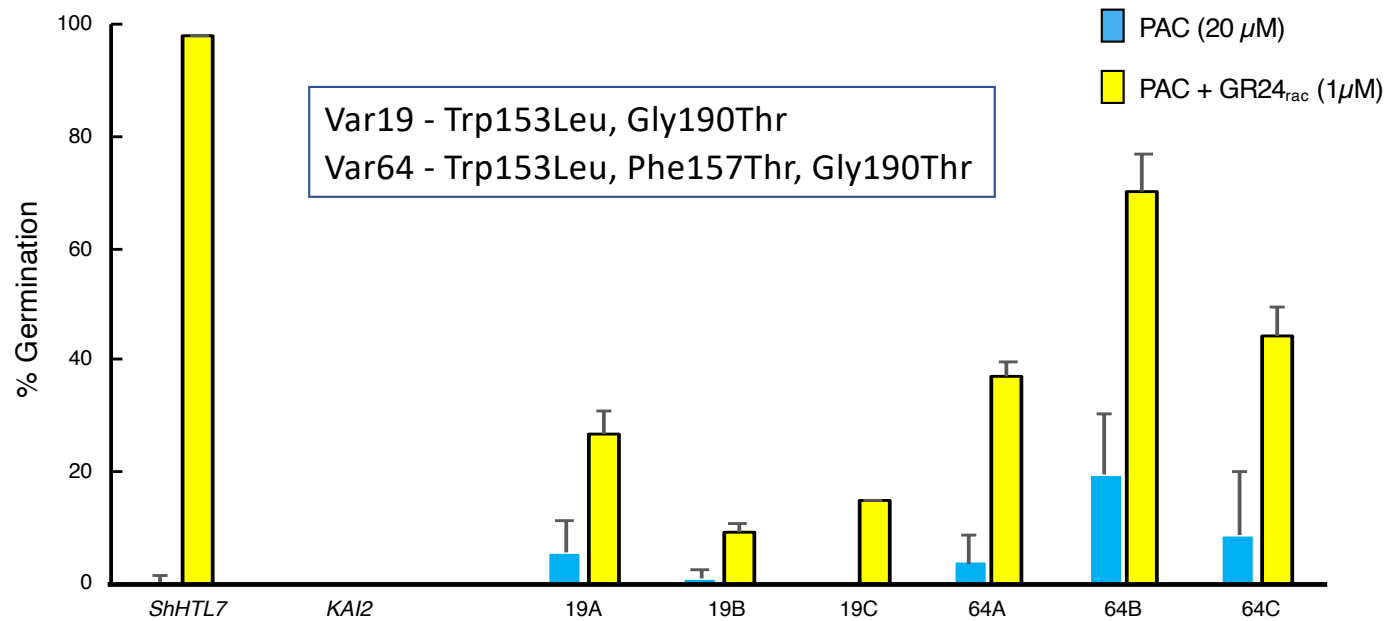


Fig. S11. SL dependent germination of mis-expressed *ShHTL7*, *KAI2*, three biologically independent Var19 lines (19A, 19B, 19C) and three biologically independent Var64 lines (64A, 64B, 64C). Each line was tested three times Bar = S.D

Table S1. Protein-ligand docking statistics

Protein	Ligand	SwissDock	AutoDock	RMSD vs 5DJ5
Var64	(2'R)-GR24	-7.02 kcal mol ⁻¹	-6.97 kcal mol ⁻¹	3.025 Å
Var64	(2'S)-GR24	-6.33 kcal mol ⁻¹	-6.39 kcal mol ⁻¹	3.100 Å
KAI2	(2'R)-GR24	-5.50 kcal mol ⁻¹	-5.41 kcal mol ⁻¹	2.901 Å
KAI2	(2'S)-GR24	-5.92 kcal mol ⁻¹	-5.84 kcal mol ⁻¹	3.148 Å

Table S2. Molecular dynamics simulations statistics

System	Convergence timepoint	Average RMSD after convergence (ligand)	Average Potential Energy
Var64 + (2'R)-GR24 #1	214 ns	0.4175 Å	-3.679 kJ/mol
Var64 + (2'R)-GR24 #2	198 ns	0.4093 Å	-3.128 kJ/mol
Var64 + (2'R)-GR24 #3	223 ns	0.4419 Å	-3.709 kJ/mol
KAI2 + (2'R)-GR24 #1	270 ns	0.9592 Å	-3.721 kJ/mol
KAI2 + (2'R)-GR24 #2	291 ns	0.9817 Å	-3.875 kJ/mol
KAI2 + (2'R)-GR24 #3	284 ns	0.9799 Å	-3.814 kJ/mol
Var64 #1	59 ns	N/A	-1.395 kJ/mol
Var19 #1	43 ns	N/A	-1.118 kJ/mol
KAI2 #1	28 ns	N/A	-1.204 kJ/mol

Table S3 Protein-Ligand Interaction Profile

Structure	Residue ID	Distance to ligand (Å)	Structure	Residue ID	Distance to ligand (Å)
DWARF14-GR24 (5DJ5)	Phe28	3.77 + 3.62	OsD14-7'carba-4BD product (5YZ7)	Phe78	3.53
	Ser97	2.40		Val148	3.85
	Val98	3.47		Phe186	3.6
	Phe126	3.72		Val194	3.99
	Phe136	3.81		Tyr209	3.91 + 4.38
	Val144	3.29		Val244	3.49
	Tyr159	3.48 + 4.02		Phe245	3.73
	Val194	3.94		Phe26	3.80
	Phe195	3.84		Ser95	2.32
	Val219	3.26		Phe134	3.71
	Ser220	3.62		Asp138	3.88
	His247	4.52 + 3.88		Leu142	3.54 + 3.83
DWARF14-CLIM (4IHA)	Phe28	3.07	Var64-(+)GR24	Thr157	3.65
	His96	5.41		Leu160	3.52
	Val98	3.94 + 2.74		Phe194	3.93
	Phe126	3.84		Leu218	3.96
	Val194	3.20		Ala219	3.99
	His247	3.31 + 3.83 + 5.01		His246	4.64

Movie S.1. The Var64 receptor displays increased flexibility and a larger binding pocket. A 1 μ s molecular dynamics simulation of KAI2 (grey) and Var64 (blue) reveals that the α E loop of Var64 presents increased motility, and its three mutations (shown in red) result in improved flexibility along the X-axis of the protein. These two factors would produce a more efficient perception of SLs as the active site opening area of Var64 is increased by 11.5 Å.

Movie S.2. Enhanced interaction between Var64 and 2'R-(+)GR24. 1 μ s molecular dynamics simulation reveals that the polar Thr190 in Var64 (blue) does a better job stabilizing the ligand than its WT counterpart. Upon binding, the α D helix of Var64 increases its movement, possibly resulting in enhanced interactions with its downstream protein partner.

Movie S.3. The WT Phe157 in Var19 directly affects the flexibility of the receptor. 0.5 μ s molecular dynamics simulation comparing the flexibility of Var19 (grey) and Var64 (blue) reveals that the presence of the WT Phe157 (grey sticks) from KAI2 produces stronger interactions between the opposite sides of the lid domain; this results in a decreased flexibility and a reduced binding pocket area, making the interaction with SL more challenging than in Var64 (variant residues shown in red sticks).